BL-11D/2019G547

Calibration of Mo/Si Multilayer Beam-splitter for Soft X-Ray Laser Beamline

Masahiko ISHINO[1,*], Thanh-Hung DINH[1], Noboru HASEGAWA[1], Masaharu NISHIKINO[1], Kazuyuki SAKAUE[2], Takeshi HIGASHIGUCHI[3], and Tadashi HATANO[4]

[1] Kansai Photon Science Institute, National Institutes for Quantum and Radiological Science and Technology, Kizugawa, Kyoto 619-0215, Japan

[2] Photon Science Center, The University of Tokyo, Bunkyo, Tokyo 113-8656, Japan

[3] Department of Electrical and Electric Engineering, Faculty of Engineering, Utsunomiya University, Utsunomiya, Tochigi 321-8585, Japan

[4] International Center for Synchrotron Radiation Innovation Smart, Tohoku University, Sendai, Miyagi 980-8577, Japan

1 Introduction

The interactions of intense short laser pulses with matter allow strong electronic excitation states and high temperatures and pressures to be created in solid materials. As a result of these interactions, the material can undergo phase and structural modifications. For instance, laser ablation, a process that removes material from the surface, is one of the direct consequences of laser pulses interacting with matter. The ablation phenomena of materials in the soft x-ray regions having pulse durations in femtosecond to nanosecond have been extensively studied for focusing property evaluations, confirmation and discussion of damage formation including estimations of thresholds, and surface machining. Especially, by use of soft x-ray free electron lasers, the interactions of ultra-short soft x-ray pulses with matter could be examined, e.g. dependences of pulse duration and/or wavelength.

Advances in physical studies and high-power laser technologies enabled us to realize laboratory-size laser-driven plasma based soft x-ray lasers (SXRLs). In our institute, the x-ray laser facility of the National Institutes for Quantum and Radiological Science and Technology (QST), the SXRL system had been developed. The SXRL beam at 13.9 nm had nearly diffraction limited divergence and full spatial coherence. The SXRL specification is as follows; Ni-like Ag laser having the wavelength of $\lambda = 13.9$ nm [1], the spectral width of $\lambda/\Delta\lambda > 10^4$, the pulse duration of τ ~7 ps [2], the beam divergence of ~0.35 mrad, and the average output energy of ~200 nJ/pulse. By use of the picosecond SXRL, we have examined ablation/damage phenomena for dielectric, insulator, metal materials and multilayer optics. The ablation threshold of lithium fluoride (LiF) crystal was lower than that of near-infrared laser or nanosecond SXRL pulses [3] and the fluence necessary to modify structures on a gold surface was essentially lower than that with optical lasers [4]. And more, threshold values and modification structures obtained by the picosecond SXRL provide the same results by the femtosecond SXRLs [5]. Another practical use of the SXRL irradiation was the development of a high-durability soft x-ray multilayer optics [6].

A critical issue in the laser system is the relatively large fluctuations of the shot-by-shot output energy. Because the SXRL is a plasma-based x-ray laser source, the output energy fluctuates. In our SXRL the variation in the output energy (pulse to pulse fluctuation) was evaluated to be 70–80 % from 15 consecutive laser shots. The fluctuation value might be large; however, the modulation of the output energy for consecutive two shots did not exceed approximately 10 % and the average of the nearest five shots was similar with a relatively small fluctuation (less than 22 %). So we estimated the output energy of the SXRL from the measured values before and after the irradiation experiments. However, in order to apply the SXRL experiment for quantitative analyses, we must correct the accurate data obtained during the experiment. Here we report the development of the SXRL beamline equipped with an intensity monitor and the efficiency measurement of the free standing Mo/Si multilayer beam-splitter (BS).

2 Instrumentation

The SXRL beamline is comprised of five parts: (1) a SXRL source, (2) an attenuator composed of zirconium (Zr) thin films, (3) an intensity monitor consisting of a free standing Mo/Si multilayer BS and x-ray charge-coupled device (CCD) camera, (4) a focusing spherical mirror with a Mo/Si multilayer coating, and (5) a sample stage. Figure 1 shows the schematic diagram of the beamline.

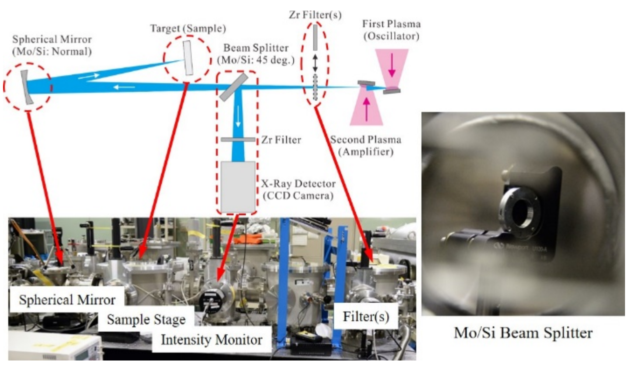

Fig. 1: Schematic diagram of the SXRL irradiation beamline and a free standing Mo/Si multilayer beam-splitter in the intensity monitor.

The spatially coherent SXRL pulse is generated from silver (Ag) plasma media using an oscillator–amplifier configuration with double Ag tape targets. The intensity of each SXRL pulse is reduced by Zr filters having thicknesses of 0.1 µm, 0.2 µm, 0.5 µm, 1 µm, or 2 µm. Zr filters may be inserted alone or in combinations in the SXRL beam axis. Moreover, filters are used for blocking the almost scattered optical or unwanted x-ray radiation from the Ag plasma media.

The intensity monitor is composed of a Mo/Si multilayer BS, Zr filters, and an x-ray CCD camera. The BS has been designed for the SXRL pulses with a wavelength of 13.9 nm and incident angle of 45°. Each SXRL pulse is divided into two beams: one is the transmitted component through the BS, which is directed toward the Mo/Si multilayer coated spherical mirror, and the other one is the reflected component, which is directed toward the x-ray CCD camera. The x-ray CCD camera records a spatial intensity profile of the SXRL beam, and serves as the intensity monitor. Zr filters installed between the BS and the x-ray CCD camera can adjust the beam intensity, so that the detection capacity of the CCD camera does not saturate. The transmittance of each Zr filter and the sensitivity of the x-ray CCD camera have been measured and evaluated using the soft x-ray beamline (BL-11D) of the synchrotron radiation facility of the Photon Factory (PF) at the High Energy Accelerator Research Organization (KEK) [7].

The SXRL pulse towards the spherical mirror is reflected and focused onto the sample surface. The mirror surface has been coated with a Mo/Si multilayer, which is optimized for soft x-rays having a wavelength of 13.9 nm at a normal incident angle. The actual incident angle of the SXRL beam with respect to the spherical mirror is near the normal (~ 1°).

The target material is set on the sample holder, which is mounted on a two-axis stage. The incident angle of the SXRL beam to the sample surface can be set freely owing to the rotation stage. To confirm the focal patterns and the best focal position, the sample can be moved along the propagation direction of the SXRL. To irradiate fresh surface areas after a prescribed number of SXRL shots, the sample can be moved perpendicular to the propagation direction.

3 Optical properties of the Mo/Si multilayer BS

To derive the irradiation energy that is sent onto the sample surface from the energy acquired by the intensity monitor, the relationship between the irradiation energy and the monitored energy has to be determined. Before evaluating the calibration ratio, the characteristic features of the Mo/Si multilayer BS must be known.

The efficiency (reflectivity and transmittance) of the Mo/Si multilayer, which has the same specifications as the equipped BS but was fabricated at a different time, was measured at the BL-11D of KEK-PF. Figure 2 shows typical efficiency curves of a Mo/Si multilayer BS. At the incident angle of 45°, the Mo/Si multilayer BS has a reflectivity around 45% and a transmittance around 10% for *s*-polarization x-rays of the wavelength region around 14 nm, including the SXRL wavelength of 13.9 nm. For the incident x-rays with *p*-polarization, nearly 40% of the incident x-rays having a wavelength within the 14 nm region are transmitted towards the spherical mirror. Due to the pseudo-Brewster angle of the Mo/Si multilayer mirror occurring around the incident angle of 45°, the reflectivity of *p*-polarization x-rays is negligible. Hence, the transmittance of *s*- and *p*-polarized x-rays are different, and the SXRL signal captured by the intensity monitor is almost entirely the reflected *s*-polarization component.

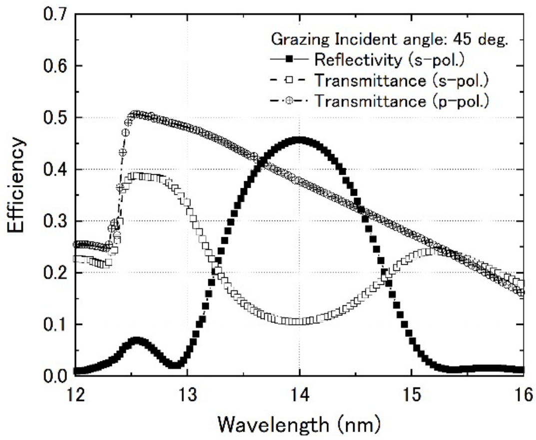

Fig. 2: Measured efficiencies of the Mo/Si multilayer BS. Efficiency curves show the reflectivity of *s*-polarized soft x-rays and the transmittance of *s*- and *p*-polarized soft x-rays. The incident angle was 45°.

In the SXRL beamline, the Mo/Si multilayer BS is set to reflect along the horizontal direction (see Fig. 1), so that the *s*- and *p*-polarizations of the SXRL beam are in accord with the vertical and horizontal components, respectively. Hence, the intensity monitor can capture just the intensity of the reflected part of the vertical component. The Mo/Si multilayer BS transmits both the vertical and horizontal components. The transmitted SXRL is focused by the spherical mirror and reaches the sample surface. Consideration of the irradiation intensity must account for both components. At the reflection by the spherical mirror, the polarization does not need to be considered, because there is no polarization dependence in the refection for the normal incidence situation.

4 Intensity calibration

To derive the irradiation intensity that is directed onto the sample surface from the detection value obtained by the intensity monitor, the relationship between the irradiation and detection intensities must be estimated. In order to measure the irradiation intensity, we put an extra Zr filter before the spherical mirror, and an extra Mo/Si multilayer–coated plane mirror and the x-ray CCD camera after the spherical mirror. The Mo/Si multilayer coating on the plane mirror has been optimized for soft x-rays of 13.9 nm at an angle of incidence of 45° so that the Mo/Si multilayer reflects the *s*-polarized component with respect to the plane mirror. Figures 3(a) and 4(a) show the experimental setup for the vertical and horizontal component measurements, respectively. When the plane mirror is set to reflect the vertical component [Fig. 3(a)], we can estimate the relative intensity of the irradiation (vertical) to monitor (vertical) components. If the plane mirror is set to reflect the horizontal component [Fig. 4(a)], the relative intensity of the irradiation (horizontal) to monitor (vertical) components can be estimated. The Zr filter was used to reduce the SXRL intensity such that it did not saturate the detection counts of the CCD camera. The reflectivity of the Mo/Si multilayer plane mirror, the sensitivity of the CCD camera, and the transmittance of the Zr filter used in the calibration experiment have also been evaluated at BL-11 of KEK-PF.

Figures 3(b) and 4(b) show the relative intensity of the vertical and the horizontal components of the SXRL pulses, respectively. The relationship between the irradiation (vertical) and the monitor (vertical) components is stable when the measurement involves SXRL pulses with the same polarization. The estimated value of the ratio between the irradiation intensity (vertical) and the monitor intensity (vertical) is 0.304±0.005. However, the dispersion between the irradiation (horizontal) and the monitor (vertical) components is relatively large, having a ratio of 0.418±0.025. Derived from the intensity measurements, the irradiation intensity directed onto the sample surface is evaluated to be (Irradiation Intensity) = (0.30 + 0.42) × (Monitor Intensity).

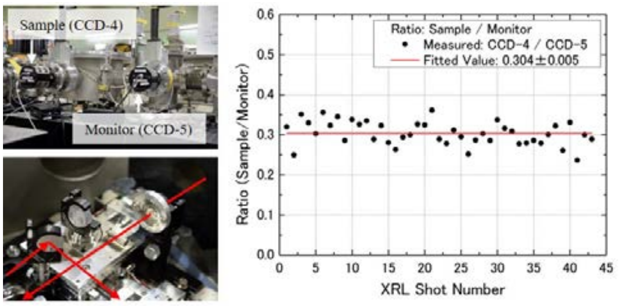

(a) (b)

Fig. 3: (a) Experimental setup for the vertical component measurement and (b) the relative intensity of the vertical component of SXRL between the irradiation intensity and the monitored intensity.

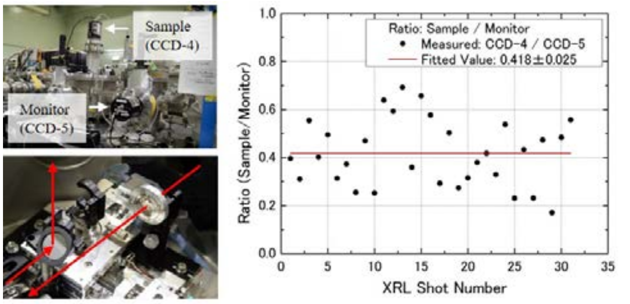

(a) (b)

Fig. 4: (a) Experimental setup for the horizontal component measurement and (b) the relative intensity of the horizontal component of SXRL between the irradiation intensity and the monitored intensity.

5 <u>Focal spot size</u>

To confirm the focusing pattern of the SXRL, a LiF crystal was used as a detector. The spatial pattern of the focusing SXRL was recorded in the LiF crystal as color centers [11]. The spatial pattern of the CCs can be detected using a fluorescence microscope. Use of the LiF crystal as a two-dimensional detector is a technique that can properly characterize the focusing beam.

Figure 5(a) shows the photoluminescence image of the CCs produced in the LiF crystal, which was set at the best focal position. Figure 5(b) shows the cross-sectional profile of the signal intensity obtained from the image along the dotted diagonal line. The size of the full width at half maximum value is 10 μm. The focal spot size of the SXRL was then estimated to be 5–6 μm in radius and the average focal area was estimated to be approximately 100 μm^2. The maximum fluence on the sample surface is around 30 mJ/cm^2, which was calculated using the obtained irradiation intensity and spot area. This value is enough to make damages on material surfaces.

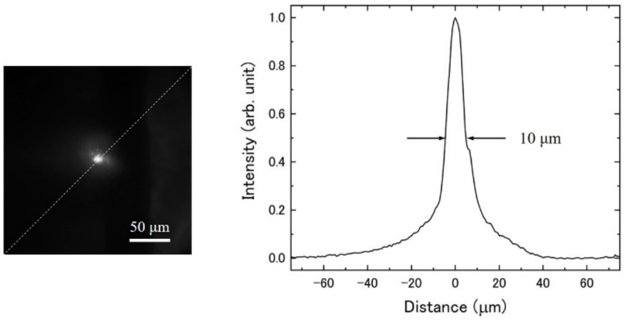

(a) (b)

Fig. 5: (a) Fluorescence microscopy image of the photoluminescence signal emitted from color centers produced in a LiF crystal irradiated by the SXRL near the optimal focal position. (b) Cross-sectional profile of the photoluminescence along the dotted diagonal line.

6 <u>Summary</u>

We have developed the SXRL beamline for surface processing and damage studies. The beamline is equipped with an intensity monitor, which provides the laser intensity directed onto the sample. To derive the irradiation energy from the energy acquired by the intensity monitor, we have evaluated the characteristic features of the Mo/Si multilayer BS, and then estimated the relationship between the irradiation and detection intensities. The SXRL is focused onto the sample by a spherical mirror and the average focal area is estimated to be approximately 100 μm^2. Therefore, the maximum fluence, calculated using the obtained irradiation intensity and spot area, is around 30 mJ/cm^2. This fluence is high enough to create ablation (damage) structures on the material surfaces.

<u>Acknowledgement</u>

Measurements of the transmittances of Zr filters, the sensitivity of the x-ray CCD camera, and the efficiency of the Mo/Si multilayer beam-splitter were performed under the approval of the Photon Factory Program Advisory Committee (Proposal Nos. 2015G667, 2017G638 and 2019G547). Part of this work is supported by JSPS KAKENHI (JP19K15402) and MEXT Q-LEAP (JPMXS0118067246, JPMXS0118070187).

References

[1] A. Ya. Faenov *et al*., *App. Phys. Lett.* **94**, 231107 (2009).
[2] M. Ishino *et al*., *Appl. Phys.* A **110**, 179 (2013).
[3] N. A. Inogamov *et al*., *J. Opt. Technol*. **78**, 473 (2011).
[4] S. Ichimaru *et al*., *Springer Proc. Phys*. **202**, 303 (2018).
[5] T.-H. Dinh *et al*., *PF Activity Report 2019* **#37**, 130 (2020).

* ishino.masahiko@qst.go.jp